Urologia Internationalis

Research Article

Urol Int 2021;105:507–513
DOI: 10.1159/000512878

Received: April 22, 2020
Accepted: November 4, 2020
Published online: February 24, 2021

Potential of Perfusion Magnetic Resonance Imaging to Predict Residual Renal Function after Radical Nephroureterectomy

Yuma Waseda[a] Soichiro Yoshida[a] Yuki Arita[b, c] Taro Takahara[c, d] Tsuyoshi Sakamoto[e] Kazutaka Saito[a] Yasuhisae Fujii[a]

[a]Department of Urology, Tokyo Medical and Dental University Graduate School, Tokyo, Japan; [b]Department of Radiology, Keio University School of Medicine, Tokyo, Japan; [c]Department of Radiology, AIC Yaesu Clinic, Tokyo, Japan; [d]Department of Biomedical Engineering, Tokai University School of Engineering, Kanagawa, Japan; [e]PixSpace Ltd., Fukuoka, Japan

Keywords

Estimated glomerular filtration rates · Diffusion-weighted imaging · Perfusion · Split renal function · Upper-tract urothelial carcinoma

Abstract

Introduction: The diffusion-weighted imaging (DWI) technique with intravoxel incoherent motion model enables the estimation of capillary blood volume as a perfusion-related parameter- (PP-) value. Therefore, the PP-value of the kidney theoretically reflects renal capillary blood volume. We analyzed the usefulness of the PP-value in estimating postoperative renal function in upper-tract urothelial carcinoma (UTUC) patients. ***Methods:*** Forty-eight consecutive patients who underwent magnetic resonance imaging before radical nephroureterectomy from 2011 to 2018 were analyzed. A PP-map displaying PP-values on a pixel-by-pixel basis was created from DWI signals (*b*-values of 0, 500, and 1,000 s/mm^2). Two readers independently analyzed the renal PP-value. DWI-based split renal function (SRF) of the intact kidney was calculated by splitting serum Cr-based preoperative estimated glomerular filtration rates (eGFRs). The predictive accuracy of the method was evaluated using renography as the reference standard. ***Results:*** Interobserver analysis revealed an excellent correlation value of 0.97. The SRF value showed a good linear correlation with the observed postoperative eGFR ($r = 0.76$, $p < 0.001$). The predictive accuracy of the DWI-based method was similar to that of the nuclear-based method. ***Conclusion:*** This DWI-based evaluation of capillary blood volume provides a noninvasive tool for predicting the postoperative renal function, thereby facilitating the management of UTUC patients.

Introduction

Renal function in patients with upper-tract urothelial carcinoma (UTUC) is affected by upper-tract obstruction, caused by UTUC, to varying degrees. Accordingly, predicting postradical nephroureterectomy (RNU) renal function prior to surgery is complicated. Enhanced prediction of perioperative changes in renal functioning has the potential to better facilitate the management of patients with UTUC.

karger@karger.com
www.karger.com/uin

Karger

Soichiro Yoshida
Department of Urology, Tokyo Medical and Dental University Graduate School
1-5-45 Yushima, Bunkyo-ku
Tokyo 113-8519 (Japan)
s-yoshida.uro@tmd.ac.jp

It has previously been reported that the radiodensity measured within the renal cortex using a dynamic CT reflects the blood volume contained within the glomeruli and peritubular capillaries [1]. Similarly, it has been shown that the radiodensity of the renal cortex was a useful tool as renography for quantitatively predicting postoperative residual renal function in UTUC patients [2]. However, patients with borderline levels of renal function for full-dose cisplatin-based combination chemotherapy typically cannot be given the contrast agent [3]. To overcome this challenge, we employed a new radiographic approach to predict postoperative renal function using diffusion-weighted imaging (DWI) that did not require the use of an image contrast agent or exposure to radiation. Intravoxel incoherent motion (IVIM) imaging can distinguish the motion of water molecules in the capillary network from pure molecular diffusion with a single DWI acquisition technique [4, 5]. Although the perfusion fraction could be calculated from DWIs with multiple low and high *b*-values, the method is not practical under the scan time constraint. Recent studies have shown that it could be equivalently assessed as a perfusion-related parameter- (PP-) value using 3 *b*-values [6, 7]. Since DWI with IVIM model enables the estimation of blood volume through the capillaries as a PP-value, the PP-value of the kidney theoretically reflects renal capillary blood volume. Therefore, we hypothesized that the percentage of the sum of bilateral renal PP-value would reflect the split renal function (SRF) of each kidney.

The aim of this study was to quantitatively predict postoperative renal function using the PP-value. ^{99m}Tc-diethylenetriaminopentacetic acid (DTPA) renography was employed as a reference to verify the predictive accuracy of the DWI-based method.

Materials and Methods

Patients

Forty-eight consecutive patients who underwent the abdominal magnetic resonance imaging (MRI) procedure that included DWI before RNU at an academic medical center from 2011 to 2018 were analyzed. A patient with an extremely thin renal parenchyma to measure due to severe hydronephrosis was excluded from this study. Comparisons between DWI- and renography-based methods were conducted using 29 patients who also underwent ^{99m}Tc-DTPA renography before RNU. No patients received neoadjuvant systemic chemotherapy. Written informed consent was obtained from all participants, and all procedures were performed in accordance with the relevant regulations and guidelines. This study was approved by the institutional ethical committee of Tokyo Medical and Dental University (approval number #1264).

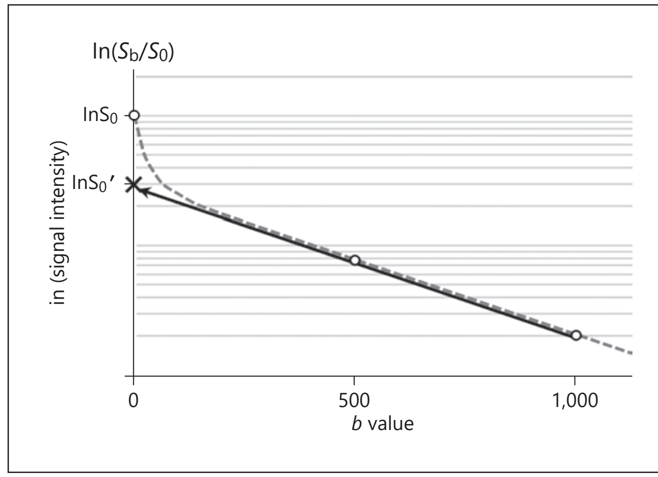

Fig. 1. The geometric method for calculating the PP-value. The dotted line represents the biexponential signal decay curve. lnS_0' was calculated as the *y*-intercept of the line through $b = 500$ and $b = 1{,}000$ s/mm^2, where S_0' represents signal intensity with pure diffusion components at $b = 0$. The PP-value was calculated from the following formula: $(S_0 - S_0')/S_0$, where S_0 equals the signal intensity at $b = 0$. PP, perfusion-related parameter.

Magnetic Resonance Imaging A multisequence MRI, including DWI, was performed using a 1.5-Tesla system (Intera Achieva; Philips, Best, The Netherlands) with a 32-channel, sensitivity-encoding body coil under free breathing conditions. The maximal gradient strength was 33 T/m, and the slew rate was 160 T/m per second. Parameters for the DWI with a single-shot, echo-planar imaging sequence were set as follows: repetition time, 1,500 ms; echo time, 65 ms; matrix, 160 × 160; field of view, 360 × 240 mm; slice thickness, 7 mm; interslice gap, 0.7 mm; and number of excitations, 3. The diffusion gradient for the DWI procedure encoded 3 orthogonal directions, and *b*-values equaled 0, 500, and 1,000 s/mm^2.

Generation of a PP -map

PP-values were determined on the basis of the biexponential fitting model for IVIM. To gain a true diffusion coefficient, we chose *b*-values of 500 and 1,000 s/mm^2 because the perfusion component may still account for a few percent of the signal even at $b =$ 400 s/mm^2 [8]. To extract perfusion contributions from DWI signals, the multistep approach was geometrically performed (Fig. 1) as follows:

1. Initially, DWI intensities using *b*-values of 500 and 1,000 s/mm^2 were plotted on a semilogarithmic chart, in which the *x*-axis represented *b*-values and the *y*-axis represented a base 10 logarithmic scale of signal intensity. The true diffusion coefficient was determined as the slope of the logarithmic regression line through the 2 points.
2. Second, lnS_0' was calculated as the *y*-intercept of the line through the 2 points, where S_0' corresponded to the signal intensity using pure diffusion components at $b = 0$.
3. Finally, PP-values, representing the perfusion fraction, were calculated using the following formula: PP-value (%) = $(S_0 - S_0')/S_0$, where S_0 is the signal intensity at which $b = 0$.

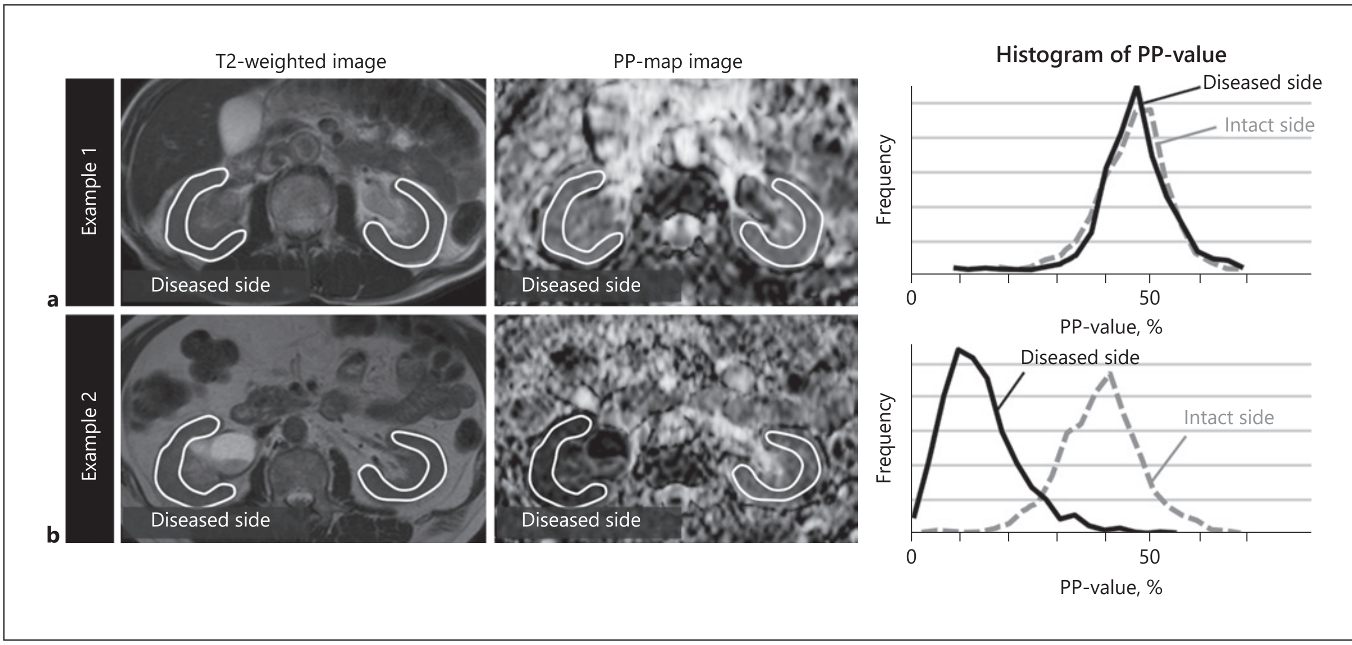

Fig. 2. Representative determinations of the renal PP-value. **a** Example 1 depicts a case in which the patient does not present with urinary obstruction. The percentage of the total renal PP-value for the intact kidney was almost 50%. The decreased rate of eGFRs after radical nephroureterectomy was high (110–66 mL/min/ 1.73 m^2). **b** Example 2 represents a case in which the patient presented with hydronephrosis. The percentage of the total renal PP-value in this case was much higher. The postoperative eGFR was almost the same as the preoperative eGFR (59 and 63 mL/min/ 1.73 m^2, respectively). PP, perfusion-related parameter; eGFR, estimated glomerular filtration rate.

The PP-value represents the perfusion fraction for each pixel, which corresponds to the percentage of voxel volume occupied by vascular and tubular structures. To establish a standard method for estimating microcirculation, we developed Attractive PP-map software (PixSpace, Ltd., Fukuoka, Japan). The software enabled us to calculate PP-values on a pixel-by-pixel basis automatically from DWI signals using *b*-values equal to 0, 500, and 1,000 s/mm^2. Moreover, 2D distributions of the PP-values were displayed as a PP-map.

Image Analysis and Calculation of Renal PP-values

Renal PP-values were calculated from a region of interest (ROI), which was manually traced to best define the renal parenchyma on the PP-map at the level of the renal hilus. The mode value of the histogram that represented pixel counts of PP-values within the ROI was adopted as the renal PP-value (Fig. 2). The T2-weighted MRIs were used as references to determine renal parenchyma areas on the corresponding PP-map images. Large cystic or tumor areas were visually identified and excluded from the ROI. A urologist (reader 1; Y.W. with 12 years of experience) and a radiologist (reader 2; Y.A. with 6 years of experience) independently analyzed the PP-values determined for each patient on both diseased and intact sides.

Evaluation of Renal Function

Estimated glomerular filtration rates (eGFRs) were calculated according to the Japanese Society of Nephrology's equation; 194 × serum Cr in mg/dL$^{-1.094}$ × age in years$^{-0.287}$ × 0.739 (if female) [9]. Preoperative and postoperative eGFR values were calculated using each patient's serum Cr measured at the timepoint nearest to preoperative imaging tests and between 1 and 3 months after RNU, respectively. PP-value-based SRF of the intact kidney was calculated by splitting preoperative eGFR using fractional renal PP-value as follows: preoperative eGFR × percentage of the total renal PP-value for intact kidney. PP-value-based SRF values were compared with observed postoperative eGFR values.

Comparing the Predictive Capacity of the PP-Value with That of Renography

Of all 48 patients, 29 patients underwent renography before RNU. Patients were manually injected with 10 mCi (370 MBq) of ^{99m}Tc-DTPA as a rapid bolus and received 20 mL saline flush. Coronal images with a pixel size of 4.8 × 4.8 mm were acquired every second for the first 60 s and every 15 s for the next 20 min. Gamma camera imaging was used to perform a renal dynamic study, and both split functions were calculated using the Gates imaging analysis protocol [10]. Nuclear SRF was calculated by multiplying the total preoperative GFR value by the fractional GFR determined by renography. The ability to predict postoperative renal function using DWI was compared with that using renography as a standard reference.

Statistical Analysis

Interobserver reliability of predicted DWI-based SRF between 2 readers was assessed using an intraclass correlation coefficient. The Pearson correlation coefficient between observed postopera-

Table 1. Clinicopathological and radiographical characteristics of 48 UTUC patients (expressed in mean and interquartile range)

	Median	Range
Gender (%)		
Male	32	(67)
Female	16	(33)
Age, years	74	(39–88)
Preoperative eGFR, mL/min/1.73 m^2	54.8	(26.3–89.2)
<60 mL/min/1.73 m^2 (%)	29	(60.4)
Postoperative eGFR, mL/min/1.73 m^2	42.3	(26.3–62.5)
<60 mL/min/1.73 m^2 (%)	47	(97.9)
<45 mL/min/1.73 m^2 (%)	29	(60.4)
Body mass index, kg/m^2	22.7	(14.0–28.8)
Smoking history (%)		
Absent	14	(29)
Present	34	(71)
Hypertension (%)		
Absent	35	(73)
Present	13	(27)
Diabetes mellitus (%)		
Absent	38	(79)
Present	10	(21)
Tumor grade (%)		
Grades 1, 2	19	(40)
Grade 3	29	(60)
pT stage (%)		
≤pT2	31	(64)
pT3,4	17	(36)
pN classification (%)		
N0	7	(15)
N+	3	(6)
Nx	38	(79)
Lymphovasucular invasion (%)		
Absent	37	(77)
Present	11	(23)
Tumor architecture (%)		
Papillary	32	(67)
Non-papillary	16	(33)
Radiographical characteristics		
Laterality (%)		
Right	23	(48)
Left	25	(52)
Tumor location (%)		
Pelvis	23	(48)
Ureter	20	(42)
Both	5	(10)
Hydronephrosis (%)		
Grades 0–2	27	(56)
Grades 3, 4	21	(44)
The percent of the total renal PP-value for intact kidney (%)		
Reader 1	57.0	(40.0–96.0)
Reader 2	55.9	(26.0–95.0)

UTUC, upper-tract urothelial carcinoma; eGFR, estimated glomerular filtration rate; PP, perfusion-related parameter.

tive eGFR and predicted DWI-based SRF was determined with a 95% confidence interval (CI) through 1,000 bias-corrected bootstrap replications of the analysis. Furthermore, a linear regression analysis was used to derive the formula used to predict postoperative eGFR. The extent to which the DWI-based method over- or underestimated postoperative eGFR values was explored graphically using a local regression and a nonparametric smoothing line derived from calibration plots. The general coherence between observed and DWI-based, predicted eGFR values was ascertained using a Bland-Altman plot.

The formula to predict postoperative eGFR using nuclear SRF was also extracted as the standard of comparison. Then, Lin's concordance correlation coefficient was further assessed to evaluate reproducibility and comparability of quantitative measurements with respect to both accuracy and precision [11]. Statistical analysis was carried out using both SPSS® version 20 software (SPSS Inc., Chicago, IL, USA) and the R-package, epiR. A two-sided p value <0.05 was considered significant.

Results

Baseline Characteristics

The median pre- and postoperative eGFR of patients were 55 and 42 mL/min/1.73 m^2, respectively (Table 1). The correlation between values was 0.71 (95% CI 0.55–0.82, $p < 0.001$). The decreased rate of perioperative eGFR was significantly higher in patients without hydronephrosis (29 vs. 6%, $p < 0.001$), lymphovascular invasion (23 vs. 5%, $p = 0.006$), and high-grade tumors (grade 3) (28 vs. 14%, $p = 0.005$). Tumor staging (≤pT2 or ≥ pT3, $p = 0.256$), age (<75 or ≥75, $p = 0.177$), diabetes mellitus ($p = 0.738$), and smoking habits ($p = 0.921$) did not produce significant differences with respect to the decreased rate of perioperative eGFR.

Development of a Formula to Predict Postoperative eGFR Using DWI

The median percentage of the total PP-value for the intact kidney determined by reader 1 and reader 2 was 57% (range: 40–96%) and 56% (26–95%), respectively. The DWI-based SRF values determined by readers 1 and 2 were 30 (17–62) and 28 (15–59) mL/min/1.73 m^2, respectively. Interobserver analysis revealed an excellent correlation of 0.97 (95% CI 0.94–0.98) between DWI-based SRF values determined by readers 1 and 2. The average DWI-based SRFs of the 2 readers showed a good linear correlation with observed postoperative eGFR values ($r = 0.76$, 95% CI 0.62–0.87, $p < 0.001$).

We applied a linear regression analysis to determine the value of the conversion factor. The regression coefficient of 1.03 (95% CI 0.77–1.29, $p < 0.001$) was determined using linear regression analysis contrasting DWI-

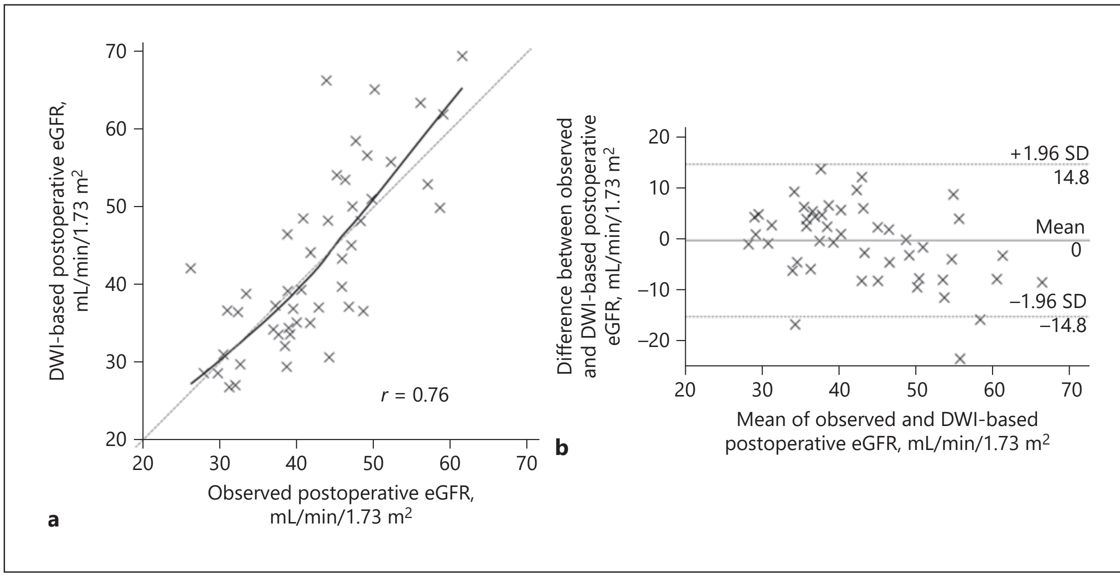

Fig. 3. a Correlation plot between predicted, DWI-based eGFR and observed postoperative eGFR values. Points estimated below the line drawn at 45° represent underpredictions. **b** Bland-Altman plots between observed and predicted eGFR values. eGFR, estimated glomerular filtration rate; DWI, diffusion-weighted imaging.

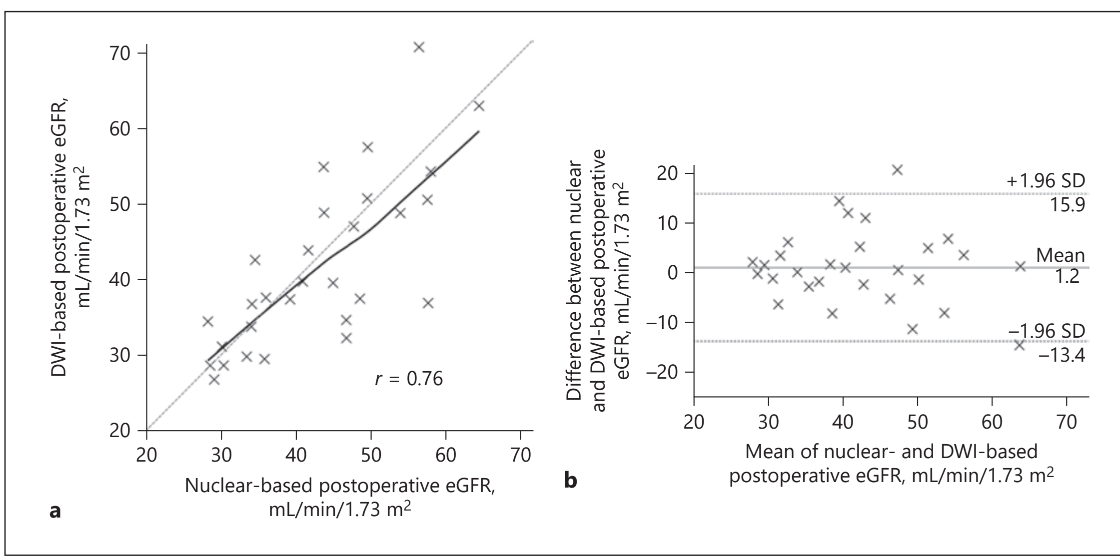

Fig. 4. Correlation (**a**) and Bland-Altman plots (**b**) between nuclear- and DWI-based predicted and estimated glomerular filtration rates. DWI, diffusion-weighted imaging.

based SRF with ascertained postoperative eGFR. Since the regression coefficient determined above was approximately 1.0, the formula for predicting the conversion factor utilized parallel translation. In this case, 10.6 was added to the DWI-based SRF value. Therefore, a DWI-based formula for predicting postoperative eGFR was determined to be as follows: postoperative eGFR = DWI-based SRF +10.6. The calibration plot in which the DWI-based prediction of eGFR was plotted against observed postoperative eGFR values showed good agreement (Fig. 3a). To verify the concordance of DWI-based predictions of eGFR with observed postoperative eGFR values, a Bland-Altman plot was created using the average of predicted and observed eGFR values as the *x*-axis and the difference between them as the y-axis. The plot revealed that the 95% CI of the bias ranged from −14.8 to 14.8 mL/min/1.73 m^2 and that the bias was almost exclusively included in the region of impaired renal function (Fig. 3b).

Comparing Predicted Postoperative eGFR Values Using DWI and Renography

The nuclear-based SRF also showed an equally significant linear correlation with observed postoperative eGFR values ($r = 0.87$, 95% CI 0.79–0.93, $p < 0.001$). Since the regression coefficient derived from a linear regression comparing the nuclear-based SRF with observed postoperative eGFR was 0.96 (95% CI 0.75–1.17, $p < 0.001$), predictive formulas were developed using parallel translation in the same way, adding a mean difference of 10.3 to the nuclear-based SRF value. The nuclear-based formula for predicting postoperative eGFR is given as follows: postoperative eGFR = nuclear-based SRF +10.3. The nuclear- and DWI-based formulas used to predict eGFR values also showed good linear correlations ($r = 0.76$, 95% CI 0.57–0.89, $p < 0.001$). The calibration and Bland-Altman plot between them are shown in Figure 4. Lin's concordance correlation coefficient between nuclear- and DWI-based predictions of eGFR values was 0.75 (95% CI 0.54–0.87) with an almost perfect bias correction factor of 0.99.

Discussion

A multimodal approach for the use of perioperative, systemic chemotherapy was considered to improve UTUC patient outcomes, since UTUC has an aggressive biology. It is, however, up for discussion whether the pre- or postoperative setting is superior for the administration of perioperative systemic chemotherapy, given our minimal capacity to predict both tumor stage and the diminishment of renal function resulting from the loss of a renal unit. This study was the first to reveal that postoperative renal function after RNU can be quantitatively predicted using preoperative DWI in UTUC patients.

In dynamic CT, the radiodensity in Hounsfield units of each pixel was reported to reflect the blood volume contained within glomeruli and peritubular capillaries in each pixel [1]. Therefore, Hounsfield units can serve as surrogate indicators of renal function, as we have previously showed [2]. However, patients who might require reductions in the dosage of cisplatin-based chemotherapy due to impaired renal functioning were often unable to be given adequate levels of radiocontrast agents [3]. With respect to MRI, Le Bihan et al. [4, 5] demonstrated that IVIM imaging could be used to quantify the levels of microcirculation within the capillary network along with molecular diffusion occurring within a single-image voxel using DWI, provided that both low and high b-values were considered. It is notable that this technique does not require injection of a gadolinium-based contrast agent and can be given to patients with renal insufficiencies or allergies to contrast agents. In the current study, our capacity to predict renal function was significant, even in patients with impaired renal function. Recently, the utility of DWI in the diagnosis of several malignancies has been increasingly reported [12, 13], and this method has the potential to facilitate the prediction of residual renal function.

The perfusion fraction can be used as a biomarker for differentiating between the diagnosis of either benign and malignant tumors in the salivary gland [14] and pancreas [15]. It was also shown to correlate with eGFR, reflecting the contribution of microcirculation in patients after transplantation [16]. Although the perfusion fraction could be theoretically estimated using a nonlinear least-square algorithm with a multiexponential signal decay curve using DWIs with various low and high b-values, significant errors were produced in spite of considerable effort and time. Recently, Sumi et al. [6] showed that it could be equivalently assessed geometrically using 3 b-values equal to 0, 500, and 1,000 s/mm^2, and another external validation study showed that this geometrically determined PP-value could facilitate the differentiation of major types of head and neck tumors [7]. Therefore, we adopted this geometric method utilizing the same 3 b-values with the report of Sumi to calculate PP-values. When a PP-value is applied to the kidney parenchyma as a renal PP-value, it has the capacity to contain information regarding urinary flow in renal tubules. Nonetheless, the percentage of the total bilateral renal PP-value could reflect SRF and be useful to quantitatively predict postoperative renal function. External radionuclide counting is considered a common way to determine SRF. The measured value itself, however, poorly correlated with postoperative renal function, and the approach of splitting the Cr-based total eGFR value would be needed [2]. In the current study, the ability to predict postoperative renal function using DWI was equal to the predictive capacity of renography.

In this study, hydronephrosis, lymphovascular invasion, and the presence of high-grade tumors were inversely associated with the perioperative decrease of eGFR values. Although the absence of hydronephrosis has been reported to be a risk factor for renal insufficiency after RNU [17, 18], evaluation using binary variables is qualitative and may not be useful in a clinical setting. This has been the first study that has been able to demonstrate that the renal PP-value calculated from DWI could reflect the preoperative SRF of an intact kidney, which facilitates the quantitative prediction of postoperative renal functioning.

Limitations of our study included its retrospective nature and our relatively small sample size. Future studies will be required to establish the usefulness of the renal PP-value to assess postoperative renal functioning in UTUC patients.

Conclusions

The percentage of the total bilateral renal PP-value for the intact kidney in preoperative DWI is indicative of the ratio of SRF, which is a useful tool for predicting the level of postoperative renal function after RNU in UTUC patients. This may also facilitate the selection of an appropriate context for cisplatin-based combination chemotherapy for UTUC patients treated with RNU.

Statement of Ethics

The Institutional Ethical Committee of Tokyo Medical and Dental University approved this retrospective study (approval number #1264). All human subjects provided written informed consent. All procedures were performed in accordance with the World Medical Association Declaration of Helsinki.

Conflict of Interest Statement

The authors have no conflicts of interest to declare.

Funding Sources

This research was supported by JSPS KAKENHI, Grant Number JP18K16687.

Author Contributions

Yuma Waseda: conceptualization, methodology, formal analysis, investigation, resources, data curation, writing – original draft, visualization, and funding acquisition. Soichiro Yoshida: conceptualization, methodology, investigation, writing – review and editing, visualization, and funding acquisition. Yuki Arita: investigation, formal analysis, and writing – review and editing. Taro Takahara: methodology and formal analysis. Tsuyoshi Sakamoto: software and methodology. Kazutaka Saito: supervision and project administration. Yasuhisa Fujii: supervision, project administration, and funding acquisition.

References

1 Dawson P, Peters AM. Functional imaging in computed tomography. The use of contrast-enhanced computed tomography for the study of renal function and physiology. Invest Radiol. 1993;28(5):S79–6.
2 Waseda Y, Saito K, Ishikawa Y, Kawano K, Yokoyama M, Ishioka J, et al. Predictive ability of renal cortex enhancement in dynamic computed tomography for residual renal function after nephroureterectomy: comparison with (99m) Tc-diethylenetriaminopentacetic acid renography and validation study. Int J Urol. 2019;26(2):266–72.
3 Weisbord SD, Mor MK, Resnick AL, Hartwig KC, Palevsky PM, Fine MJ. Incidence and outcomes of contrast-induced AKI following computed tomography. Clin J Am Soc Nephrol. 2008;3(5):1274–81.
4 Le Bihan D, Breton E, Lallemand D, Aubin ML, Vignaud J, Laval-Jeantet M. Separation of diffusion and perfusion in intravoxel incoherent motion MR imaging. Radiology. 1988;168(2):497–505.
5 Le Bihan D, Turner R. The capillary network: a link between IVIM and classical perfusion. Magn Reson Med. 1992;27(1):171–8.
6 Sumi M, Nakamura T. Head and neck tumors: assessment of perfusion-related parameters and diffusion coefficients based on the intravoxel incoherent motion model. AJNR Am J Neuroradiol. 2013;34(2):410–6.
7 Sasaki M, Sumi M, Eida S, Katayama I, Hotokezaka Y, Nakamura T. Simple and reliable determination of intravoxel incoherent motion parameters for the differential diagnosis of head and neck tumors. PLoS One. 2014;9(11):e112866–e66.
8 Le Bihan D. What can we see with IVIM MRI? Neuroimage. 2019;187:56–67.
9 Matsuo S, Imai E, Horio M, Yasuda Y, Tomita K, Nitta K, et al. Revised equations for estimated GFR from serum creatinine in Japan. Am J Kidney Dis. 2009;53(6):982–92.
10 Gate F. Glomerular filtration rate: estimation from fractional renal accumulation of 99mTc-DTPA (stannous). AJR Am J Roentgenol. 1982;138(3):565–70.
11 Lin LI. A concordance correlation coefficient to evaluate reproducibility. Biometrics. 1989;45(1):255–68.
12 Yoshida S, Masuda H, Ishii C, Saito K, Kawakami S, Kihara K. Initial experience of functional imaging of upper urinary tract neoplasm by diffusion-weighted magnetic resonance imaging. Int J Urol. 2008;15(2):140–3.
13 Sudah M, Masarwah A, Kainulainen S, Pitkanen M, Matikka H, Dabravolskaite V, et al. Comprehensive MR urography protocol: equally good diagnostic performance and enhanced visibility of the upper urinary tract compared to triple-phase CT urography. PLoS One. 2016;11(7):e0158673–e73.
14 Sumi M, Van Cauteren M, Sumi T, Obara M, Ichikawa Y, Nakamura T. Salivary gland tumors: use of intravoxel incoherent motion MR imaging for assessment of diffusion and perfusion for the differentiation of benign from malignant tumors. Radiology. 2012;263(3):770–7.
15 Lemke A, Laun FB, Klauss M, Re TJ, Simon D, Delorme S, et al. Differentiation of pancreas carcinoma from healthy pancreatic tissue using multiple b-values: comparison of apparent diffusion coefficient and intravoxel incoherent motion derived parameters. Invest Radiol. 2009;44(12):769–75.
16 Eisenberger U, Thoeny HC, Binser T, Gugger M, Frey FJ, Boesch C, et al. Evaluation of renal allograft function early after transplantation with diffusion-weighted MR imaging. Eur Radiol. 2010;20(6):1374–83.
17 Hoshino K, Kikuchi E, Tanaka N, Akita H, Ito Y, Miyajima A, et al. Preoperative hydronephrosis: Independent predictor for changes in renal function following nephroureterectomy. Jpn J Clin Oncol. 2012;42(3):202–7.
18 Fang D, Zhang Q, Li X, Qian C, Xiong G, Zhang L, et al. Nomogram predicting renal insufficiency after nephroureterectomy for upper tract urothelial carcinoma in the Chinese population: exclusion of ineligible candidates for adjuvant chemotherapy. Biomed Res Int. 2014;2014:529186.